

Calculation of Optical Constants of Ta₂O₅ Thin Film

Dr. P. Laveena Manjulatha

Asst Proff of Physics, Department of Physics, Vivekananda Govt Degree College(A), Vidyanagar ,
Hyderabad,TG, India-500044.

Abstract:

The optical constants of tantalum pentoxide thin films, including refractive index(n), extinction coefficient (k), and absorption coefficient (α), play a crucial role in the design of optical coatings, waveguides, and sensors, in this study, thin films were fabricated using a pulsed laser deposition (pld) technique on glass substrates. The films thickness morphology and optical properties were systematically analyzed. Spectroscopic ellipsometry (se) and UV-Vis spectrophotometer. Based on these experimental data, key optical constants such as refractive index(n), extinction (α) were determined using appropriate theoretical models and equations.

The refractive index was found to vary with wavelength, showing normal dispersion behaviour, while the extinction coefficient remained low in the visible region, indicating high transparency of the films. The optical band gap was also estimated using Tauc's plot, confirming the insulating nature of Ta₂O₅. Film thickness and surface uniformity were considered in the analysis to improve the accuracy of calculated constants. The results demonstrate that Ta₂O₅ thin films possess desirable optical characteristics, making them suitable for applications in anti-reflective coatings, optical filters and wave guides.

Keywords: Tantalum pentoxide, thin films, optical constants, refractive index, extinction coefficient, spectroscopic ellipsometry, pulsed laser deposition.

Introduction

Tantalum Oxide (Ta₂O₅) thin films, by virtue of its commendably high refractive index and static dielectric constant [1], find applications in surface wave acoustics waveguides, transistors, optical displays and photovoltaic devices [2]. Further Ta₂O₅ is chemically robust in the harsh environment [3] due to which its thin films are utilized as protective coating. The insulating devices, which require high permittivity material, employ thin films of Ta₂O₅. Other properties, such as lower thermal stress and excellent environmental durability, are also exploited for applications [4,5]. To grow thin films on different substrates, one can employ different variants of physical vapor deposition technique (atomic layer deposition, thermal evaporation, e- beam evaporation and ion assisted evaporation coating technique) [6, 7] or Chemical vapor deposition technique (Microwave plasma enhanced technique, spray pyrolysis, sol-gel technique) [8,9]. The microstructure and electrochemical properties of thin layers are affected by coating technique used [10]. Thermal is one of the oldest techniques for fabrication of thin films but suffers due to defects of material segregation and precipitation, which degrade the properties of thin films (See Section 2.1.2) [10]. E-beam evaporation technique was preferred to fabricate thin films as

it yields uniform coating with good adhesion. The parameters such as pre-treatment of the substrate, temperature and pressure of chamber, partial pressure of oxygen, and thickness of coating material play a vital role in governing the quality of deposited thin film. This mandates the conceptual understanding of conditions maintained during the process of deposition and variation of optical parameters while designing a device. The selection of material is entirely based on suitability to the required application. The transmission and other optical characteristics of thin films are governed by its optical parameters and thickness [11, 12] and hence play a decisive role in the performance of thin film based devices [13, 14]. Among the above parameters, thickness of the coating material plays a vital role for the desired outcome. Although coating equipment have in-built thickness monitor, but in case of its failure non-availability), it is challenging to calculate the thickness of fabricated thin film. Numerous methods, such as Kramer–Kronig [15], classical oscillator [16], Swanepoel’s Envelope method [17], are used to calculate the optical constants. Reflection or absorption spectra are utilized in some of these theoretical formulations while others require transmission spectrum. In case of bulk materials, Kramers- Kronig method is preferred despite its compromise with accuracy. On the other hand, classical Oscillator method involves tedious calculations and is discouraged. Swanepoel’s envelope method is comparatively a simple approach for evaluation of optical parameters utilizing the transmission spectrum [18-21]. There are some previous reports available regarding theoretical calculations of optical constants of Ta₂O₅ coating [22-24]. Wang et al. [22] calculated the optical constants of Ta₂O₅ thin films by using the transmittance profile method, which is suitable for material showing low optical absorption but is aided by tedious calculations. Prachachet et al. [23] utilized the transmission curve to calculate thin film thickness and optical constants by Swanepoel’s method and spectroscopic ellipsometry. Amotchkina et al. [24] measured transmittance data to calculate refractive index, thickness of layer by analyzing oscillations in transmission profile.

Refractive index and thickness of thin films are measured by m-lines method and ellipsometry [25-28]. However, due to non-availability of experimental set-ups for aforementioned measurements, optical constants and thickness of films were evaluated theoretically. This chapter provides the analysis of optimizing the coating parameters (chamber pressure, degassing time, substrate temperature, degassing voltage etc.) for uniform deposition of thin films. Subsequently, e-beam evaporation technique was used to deposit the Ta₂O₅ thin films on the optical grade glass substrates. Secondly, the optical constants such as refractive index, extinction coefficient, absorption coefficient and thickness were calculated theoretically using Swanepoel’s envelope method. The results, so obtained, were compared with corresponding values available in the literature [22-24] and found to exhibit agreement within 6-9 %. The Drop shape analyzer was used to measure the contact angle to deduce the nature (hydrophobic or hydrophilic) of thin films.

Deposition of Ta₂O₅ thin film

Mono-layers of different thickness of Ta₂O₅ material were deposited using e-beam evaporation coating technique using Pfeiffer Vacuum (Model PLS 570) deposition system (discussed in Section 2.2.3). The optical grade glass (BK7) substrates of size (40 mm x 40 mm) were used for the deposition. Different thin films (thickness = 300, 400, 500, 600 and 700 nm) were deposited by maintaining the same partial pressure of oxygen, base pressure and substrate temperature. The deposition parameters, used for the coating process, are depicted in the Table 3.1.

Table3.1: Deposition Process Parameters

S.No	Deposition Parameters	Corresponding values
1	Substrate Temperature	250°C
2	Initial base pressure	2.5x10 ⁻⁵ mbar
3	Oxygen gas Pressure	2x10 ⁻⁴ mbar
4	Deposition Rate	0.308 nm/sec
5	Substrate rotation	20 rpm

As the properties of the thin films are highly sensitive to the contaminations, the substrate was cleaned, prior to the deposition process, using ex-situ ultrasonication method in the acetone medium. The removal of surface contaminations subsequently yields high quality coating with good adhesion on the substrate. The substrate was further cleaned using the glow discharge method, which involved the evacuation of chamber to the pressure of 2.5 x 10⁻⁵ mbar and subsequent introduction of Argon gas (at a pressure of 2 x 10⁻³ mbar) into the chamber for duration of 3 minutes while maintaining a steady current of 150 m A. A degassing voltage was applied inside the chamber to evaporate impurities present in the chamber and on the surface of the crucible. The crucible was covered by the shutter to avoid undue deposition on the substrate. Usually, the degassing voltage is maintained lower than the evaporating voltage of the material to prevent the evaporation of the coating material itself. This process results in the fluctuation of chamber pressure owing to degassing. Each material requires a particular voltage and specific degassing time, depending on its acoustic impedance and molecular structure. A uniform rate of deposition is difficult to achieve in absence of prior degassing. Subsequent to the cleaning of substrate and degassing of various parts of chamber, thin film of Ta₂O₅ was deposited in the oxygenated environment by maintaining its constant flow rate at pressure of 2 x 10⁻⁴ mbar with the help of automatic gas control (RVC 300). The oxygenated environment in the chamber helps in maintaining the desired stoichiometry during growth of the film. In-situ quartz crystal monitor (Intellimetrics, IL 820) was used to control thickness during coating process.

Study of optical constants of Ta₂O₅ thin film

The optical properties (refractive index, absorption coefficient and extinction coefficient) were evaluated for Ta₂O₅ material and further used to deduce the thickness of film. A transmission spectrum of Ta₂O₅ was measured in the wavelength range of 300–1000 nm using UV-Vis-NIR spectrophotometer (Cary 7000 UMA, Agilent discussed in section 2.3.1). Swanepoel’s Envelope method was used to interpret the thickness and optical constants from the obtained transmission spectra. The calculated thickness was compared with the measured values obtained using quartz crystal thickness monitor, and it was found to agree within 1.6 %.

Estimation of optical constants and thickness by envelope method

Monolayer films of various thickness (d = 300, 400, 500, 600 and 700 nm) were coated on glass substrates. Transmission spectra, of thin films of different thickness, are represented in Figures 3.1 (a-d).

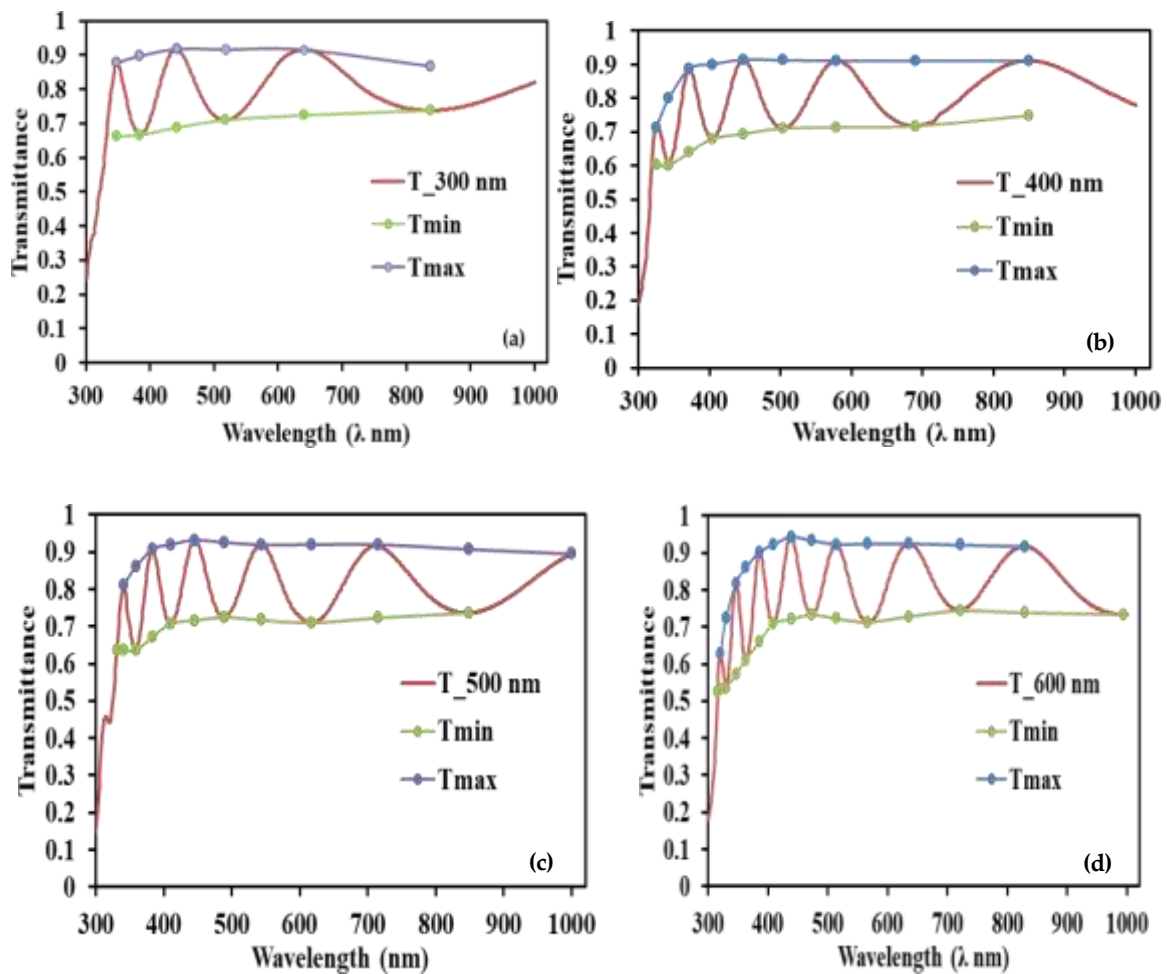


Figure3.1: Transmission Spectra of Ta₂O₅films of thickness(a)300nm(b)400 nm (c) 500 nm (d) 600 nm.

To estimate the optical constants and thickness, interference fringes in the transmission spectra were used. The interference effect induces transmission intensity oscillations (See Figure 3.1) which are purely dependent on the refractive index and thickness. Numbers of oscillations are observed to increase with the refractive index [21, 29-32]. In all the Figures 3.1 (a-d), transmission spectra were confined in envelopes to represent maxima (T_M) and minima (T_m) of interference patterns. For each wavelength, there is particular value for maxima and minima. The final refractive index (n) of the film can be estimated using Equations (3.1) and (3.2) [17, 29-32]. The intermediate refractive index is represented by “ N ” which is used to simplify the Equation (3.2). For other films, similar process was followed to calculate thickness and optical constants for the deposited substrates where T_m and T_M are minima and maxima transmission intensity values at certain wavelength (λ). The refractive index of the bare substrate is represented by s . Table 3.2 (a-d) represents the values obtained in the refractive index and thickness calculation for coated films of different thickness (300,400,500,600 nm). The Equation (3.3) was used for the calculation of thickness d_1 . The values at the initial lower range of wavelengths were neglected due to the wider deviation from general trend owing to greater absorption. The interference order (m) was calculated using equation (3.4) for each pair of λ . In the Table3.2, Equation (3.4) [20] was used to calculate m_0 . Average value of thicknesses is represented by d_1 in Table 3.2 (a-d). m_0 values are rounded off to the nearest integer to obtain the m values. For each pair of λ and n_1 , d_2 values are calculated by

using these values. For the n_2 curve fitting, Cauchy relation was used to calculate the true refractive index values (n_{true}) from Equation 3.5 [30] which is shown in the Table 3.2 (a-d).

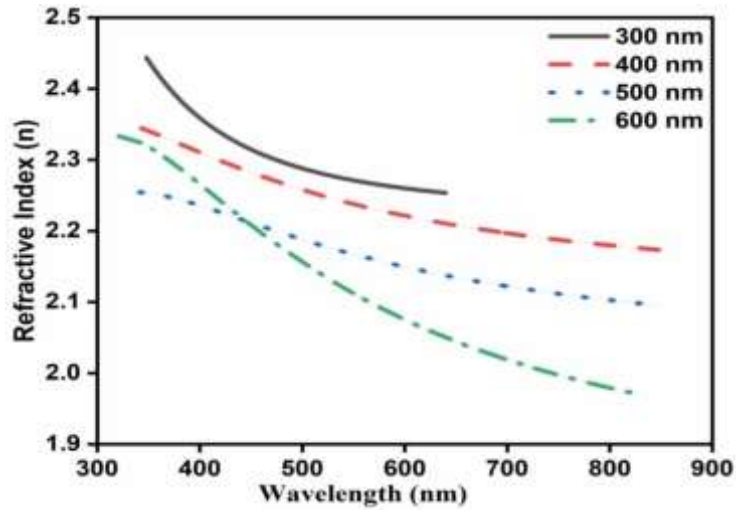


Table3.2(a):Optical constants calculation data for 300nm thickness

λ (nm)	T_M	T_m	s	n_1	Rounded d_1 (nm)	m (rounded off)	Rounded d_2 (nm)	n_2	n_{true}
838	0.8672	0.7378	1.52	1.9889	-	1.0	211	1.474	-
640	0.9152	0.7236	1.52	2.1361	272	2.0	300	2.252	2.253
518	0.9162	0.7094	1.52	2.1816	285	2.5	297	2.278	2.281
442	0.9172	0.6876	1.52	2.2511	287	3.0	294	2.333	2.320
384	0.8972	0.6659	1.52	2.2852	358	3.5	294	2.365	2.379
348	0.8773	0.6627	1.52	2.2587	-	4.0	308	2.449	2.444
332	-	0.6595	1.52	-	-	-	-	-	-
							284		

Table3.2(b): Optical constants calculation data for 400 nm thickness

λ (nm)	T_M	T_m	s	n_1	Rounded d_1 (nm)	m (rounded off)	Rounded d_2 (nm)	n_2	n_{true}
850	0.9111	0.7486	1.52	2.0519	-	2.0	414	2.174	2.173
690	0.9112	0.7175	1.52	2.1473	380	2.5	402	2.206	2.199
579	0.9114	0.7139	1.52	2.1587	414	3.0	402	2.221	2.228
503	0.9129	0.7103	1.52	2.1727	405	3.5	405	2.251	2.257
448	0.9144	0.6947	1.52	2.2240	401	4.0	403	2.291	2.283
404	0.9010	0.6791	1.52	2.2491	366	4.4	395	2.273	2.308
372	0.8876	0.6398	1.52	2.3550	413	5.0	395	2.378	2.328
343	0.7999	0.6006	1.52	2.3250	6959	5.3	391	2.325	2.344
325	0.7123	0.6026	1.52	2.0808	-	5.0	390	2.078	-

319	-	0.6047	1.52	-	-	-	-	-	-
							400		

Table3.2(c): Optical constants calculation data for 500 nm thickness

λ (nm)	T_M	T_m	s	n_1	Rounded d_1 (nm)	m (rounded off)	Rounded d_2 (nm)	n_2	n_{true}
1000	0.8948	-	1.52	-	-	1.0	-	0.992	-
848	0.9073	0.7360	1.52	2.0827	-	2.5	509	2.103	2.095
715	0.9199	0.7229	1.52	2.1472	459	3.0	499	2.128	2.119
617	0.9197	0.7098	1.52	2.1869	509	3.5	494	2.142	2.144
543	0.9196	0.7171	1.52	2.1643	581	4.0	502	2.155	2.170
489	0.9259	0.7244	1.52	2.1538	534	4.5	511	2.183	2.193
445	0.9322	0.7160	1.52	2.1905	527	5.0	508	2.207	2.214
410	0.9202	0.7076	1.52	2.1946	487	5.4	504	2.196	2.231
384	0.9083	0.6722	1.52	2.2843	457	6.0	504	2.286	2.243
359	0.8601	0.6369	1.52	2.3145	917	6.5	504	2.315	2.251
341	0.8120	0.6365	1.52	2.2144	-	6.5	500	2.199	2.254
331	-	0.6361	1.52	-	-	-	-	-	-
							504	-	

Table 3.2(d):Optical constants calculation data for 600nm thickness

λ (nm)	T_M	T_m	s	n_1	Rounded d_1 (nm)	m (rounded off)	Rounded d_2 (nm)	n_2	n_{true}
994	-	0.7337	1.52	-		2.0	-	1.744	1.970
829	0.9177	0.7386	1.52	2.0954	-	2.8	554	2.036	2.009
721	0.9211	0.7435	1.52	2.0873	594	3.0	518	1.897	2.053
635	0.9245	0.7281	1.52	2.1399	521	3.8	564	2.117	2.099
567	0.9239	0.7128	1.52	2.1854	609	4.4	571	2.188	2.143
514	0.9234	0.7228	1.52	2.1539	742	4.7	561	2.119	2.183
473	0.9331	0.7329	1.52	2.1417	618	5.0	552	2.074	2.221
439	0.9429	0.7209	1.52	2.1946	597	5.7	570	2.195	2.255
409	0.9222	0.7089	1.52	2.1942	506	6.0	559	2.152	2.281
386	0.9016	0.6604	1.52	2.3110	398	6.8	568	2.302	2.306
363	0.8601	0.6119	1.52	2.4038	442	7.5	566	2.388	2.321
347	0.8187	0.5737	1.52	2.4705	693	8.1	569	2.466	2.331
330	0.7240	0.5355	1.52	2.4234	-1153	8.4	572	2.432	2.333
321	0.6293	0.5306	1.52	2.1461	-	7.6	568	2.140	-
316		0.5257	1.52	-	-		-	-	
							561		

The thickness calculations by envelope method in case of (d= 300 , 400 and 500 nm) exhibit good agreement as compared to greater thickness (d =.600 nm).The thickness of different film as measured by quartz crystal monitor and those evaluated through Swanepoel’s Envelope method are tabulated below

Table3.3:Comparison data for thickness calculated

d_1 (measured)(innm)	d_2 (evaluated)(innm)	$\%Error = \frac{d_2 - d_1}{d_1} \times 100$
300	284.0	-5.63
400	399.6	-0.10
500	503.5	0.70
600	560.9	-6.51

Figures 3.2 shows the refractive index profile of different coated substrates. The refractive indices profiles are observed to follow the normal dispersion curve. The refractive index of the films of thickness (300, 400 and 500 nm) were validated by Reflectometer (F10-RT,Reflectometer).The theoretically evaluated refractive index of thickness 600 nm departures by ~7 % from that measured with reflectometer so further investigations are preferred with films of lower thickness (300, 400 and 500 nm). The validation data for refractive index values are shown in the Figure 3.3.

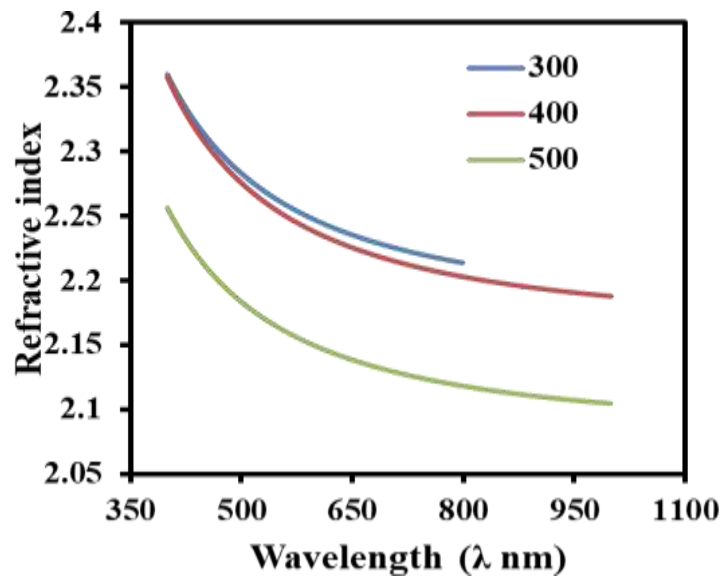


Figure 3.3: Validation of refractive index by Reflectometer (thickness 300, 400 and 500 nm)
 Comparison of estimated refractive index values are shown in the Table 3.4.

Table3.4: Comparison of the estimated refractive index

Samples(set thickness)	Refractive Index by envelope method	Refractive Index by Reflectometer
300 nm	2.27	2.26
400 nm	2.19	2.25
500 nm	2.12	2.16

Absorption Coefficient (α) was calculated by using Equation 3.6 in which deposited film. The plot in Figure 3.4 (a, b) shows the spectral variation of extinction coefficient and absorption coefficients. The extinction coefficient falls with increasing wavelength owing to scattering and absorption process.

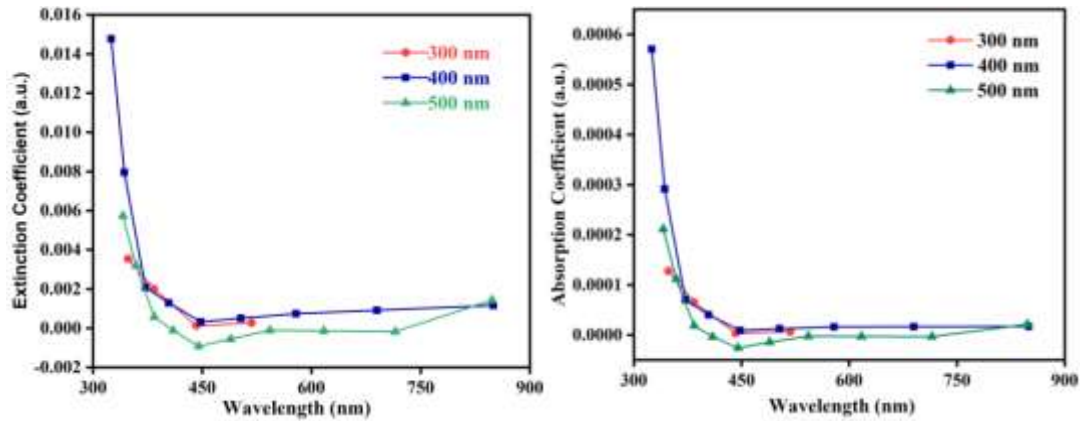


Figure3.4: Spectral variation of extinction and absorption Coefficient of Ta₂O₅

Conclusion : Characterization Techniques

Coherence Correlation Interferometry

Thickness and step height measurement was performed with the help of this coherence correlation interferometry technique (See Section 2.3.3) which is based on the superposition principle. Light from the source is divided into two parts using a beam splitter. One of these forms the reference beam while other is used to scan the sample surface. When the scan of the sample is completed, these beams are compared to create the surface profile of the sample. Coated Samples of thickness (300,400 and 500 nm) were analyzed with this technique and surface map of 300 nm thickness sample, so obtained, is shown in the Figure 3.5. The maps clearly depict the uncoated and coated surfaces (labeled 1 and 2 respectively).

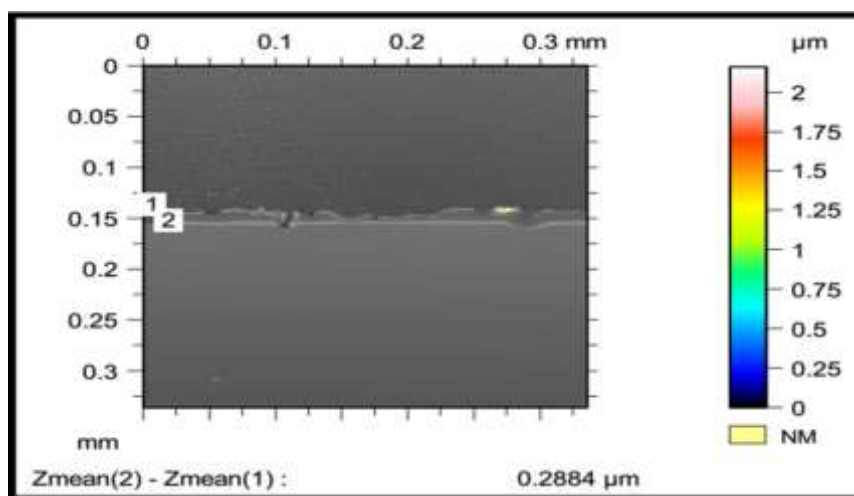


Figure3.5: Surface Map of Ta₂O₅ thinfilm of 300nm thickness

Table 3.5 shows the error calculation in estimated thickness, quartz crystal thickness and thickness observed by CCI (Coherence-Correlation Interferometer) technique.

Thickness measured by quartz crystal monitor is in good agreement with those evaluated using Swanepoel’s method. The thickness of deposited films, as measured by CCI technique are in agreement with the in-situ thickness measurements within an error of ~ 4%.The differences in two values may possibly be attributed to the distance between the substrate holder and quartz crystal position in the chamber which is accounted by introducing tooling factor. Tooling factor is defined as ratio of distance between the substrate holder and source to that between quartz crystal and source.

Table3.5: Comparison of Calculated thickness versus CCI thickness

Samples	Set Thickness	Estimated Thickness using envelope method	Estimated thickness using CCI technique	%Error using envelope method	%Error using CCI technique
1	300 nm	284.0 nm	288 nm	5.63	4.0
2	400 nm	399.6 nm	385 nm	0.10	3.8
3	500 nm	503.5 nm	479 nm	0.70	4.0

Drop Shape Measurements

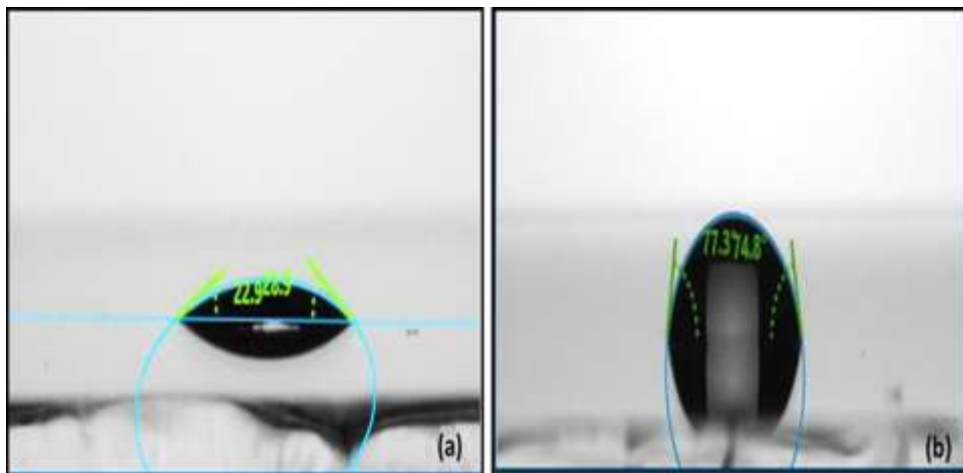


Figure3.6:Contact angle measurement of (a) are glass substrate (b) Coated film of thickness 300 nm.

Drop Shape Analyzer (DSA 100E, Kruss, USA) (See Section 2.3.4) was used to measure the contact angle of the coated film at the interface with substrate, to assign hydrophilic or hydrophobic nature of substrate, for various applications for display systems (such as automobiles as self-cleaning property. A sessile drop of distilled water was poured above the coated substrate to know the contact angle of substrate with water. The contact angle of the drop with bare substrate was compared with the contact angle of the coated substrate with thin film thickness which is shown in the Figure 3.6. It was observed that the contact angle in case of bare substrates was about 22° while in case of 300, 400 and 500 nm coated substrates it was 77, 85 and 89° respectively which indicates the hydrophobic nature of the tantalum oxide thin films. Hence, hydrophobic nature of this material can be used in the areas where water repellent surface is required.

Acknowledgement

Author is thankful to the department of physics for conduction of research work ,Extend thanks to the Nano physics lab , New Delhi.

References

1. Optical properties and microstructure of Ta₂O₅ biaxial film Qi H, Xiao X, He H, Yi K, Fan Z. *Applied Optics*,(2009), **Vol.48(1)**,pg. 127-33.
2. Tantalum pentoxide(Ta₂O₅) thin films for advanced dielectric applications Chaneliere C, Autran J, Devine R, Balland B. *Materials Science and Engineering: R: Report*,(1998), **Vol.22(6)**,pg.269-322.
3. Tantalum oxide thin films as protective coatings for sensors. Christensen C, De Reus R, Bouwstra S. *Journal of Micromechanics and Microengineering*,(1999), **Vol.9(2)**, pg.113.
4. Properties of tantalum oxide thin film for solid electrolyte. Saito T, Ushio Y, Yamada M, Niwa T. *Solid State Ionics*,(1990), **Vol. 40**,pg. 499-501.
5. Ionic conductivity of tantalum oxide films prepared by sol-gel process for electrochromic devices. Ozer N, He Y, Lampert CM In *Optical Materials Technology for Energy Efficiency and Solar Energy Conversion XIII*, International Society for Optics and Photonics, (1994), **Vol. 2255**, pg. 456-466.
6. Electrical and optical properties of vacuum-evaporated indium-tin oxide films with high electron mobility Nagatomo T, Maruta Y, Omoto O. *Thin Solid Films*, (1990), **Vol.192(1)**,pg. 17-25.
7. Characteristics of indium tin oxide films deposited by RF magnetron sputtering. Joshi R, Singh V, McClure J. *Thin Solid Films*, (1995), **Vol.257(1)**,pg. 32-35.
8. Photocatalytic TiO₂ deposition by chemical vapor deposition. Ayun D, Jin Y, Kim B, Lee JK, Park D. *Journal of Hazardous Materials*,(2000), **Vol. 73(2)**,pg. 199-206.
9. Sol-gel derived, air-baked indium and tin oxide films Mattox DM. *Thin Solid Films*, (1991), **Vol.204(1)**, pg. 25-32.
10. A comparative study on IrO₂-Ta₂O₅ coated titanium electrodes prepared with different methods. Xu L, Xin Y, Wang J. *Electrochimica Acta*,(2009), **Vol.54(6)**,pg.1820-1825.
11. Design of reproducible polarized and non-polarized edge filters using genetic algorithm Ejigu EK, Lacquet BM. *Journal of Optics*,(2010), **Vol. 12(3)**,pg. 035401.
12. Optical thin film optimization design using genetic algorithms. Li DG, Watson AC. *IEEE-International Conference on Intelligent Processing Systems (Cat.No. 97TH8335)*, (1997), **Vol. 1**, pg. 132-136
13. Structural and optical properties of nano-spin coated sol-gel porous TiO₂ films. El-Nahass, M., M. Ali, and A. El-Denglawey *Transactions of Nonferrous Metals Society of China*,(2012), **Vol.22(12)**,pg. 3003-3011
14. Structural and optical properties of TiO₂ thin films prepared by spin coating. *Journal of sol-gel science and technology* StaI, J lassi M, Hajji M, Boujmil MF, Jerbi R, Kandyla M, Kompitsas M, Ezzaouia H. *Journal of Sol-Gel Science and Technology*,(2014), **Vol.72(2)**,pg. 421-427.
15. Improved thickness estimation of liquid water using Kramers-Kronig relations for determination of precise optical parameters in terahertz transmission spectroscopy. Son H, Choi D H, Park G S *Optics Express*, (2017), **Vol.25(4)**,pg. 4509-4518.
16. Determination of the optical constants of MgF₂ and ZnS from spectrophotometric measurements and the classical oscillator method. Siqueiros JM, Machorro R, Regalado LE *Applied Optics*,(1988), **Vol.27(12)**,pg. 2549-1553.

17. Determination of surface roughness and optical constants of inhomogeneous amorphous silicon films. Swanepoel R. Journal of Physics E: Scientific Instruments, (1984), **Vol.17(10), pg. 896.**
18. The determination of the thickness and optical constants of the ZnO crystalline thin film by using envelope method. Caglar M, Caglar Y, Ilcan S. Journal of Opto electronics and Advanced Materials, (2006), **Vol.8(4), pg. 1410.**
19. Determination of the thickness and optical constants of metal oxide thin films by different methods. Gholami M, Nazari A, Azarin K, Yazdanimheher S, Sadeghniya B. Journal of Basic and Applied Scientific Research, (2013), **Vol.3(5), pg. 597-600.**
20. Validity of Swanepoel's method for calculating the optical constants of thick films Shaaban ER, Yahia IS, El-Metwally EG. Acta Physica Polonica-Series A General Physics, (2012), **Vol.121(3), pg. 628.**
21. Practical design and production of optical thin films. Editor. CRC press, (2002).
22. Method for calculating optical constants of weakly absorbing coatings. Wang G, He S, Bai Y, Li W, Zhang J, Zhou Y. Laser physics, (2019), **Vol. 30(1), pg. 016206.**
23. Investigation of optical characteristics of the evaporated Ta₂O₅ thin films based on ellipsometry and spectroscopy Prachachet R, Buranasiri P, Horprathum M, Eiamchai P, Limwichean S, Nuntawong N, Chindaudom P, Samran suksamer B, Lertvanith phol T. Materials Today: Proceedings, (2017), **Vol.4(5), pg. 6365-6371**
24. Oscillations in spectral behavior of total losses (1-R-T) in thin dielectric films Amotchkina TV, Trubetskoy MK, Tikhonravov AV, Janicki V, Sancho-Parramon J, Razskazovskaya O, Pervak V. Optics Express, (2012), **Vol.20(14), pg. 16129-44.**
25. Method for calculating optical constants of weakly absorbing coatings. Wang G, He S, Bai Y, Li W, Zhang J, Zhou Y. Laser Physics, (2019), **Vol. 30(1), pg. 016206.**
26. Calculation of the thickness and optical constants of lead titanate thin films grown on MgO from their transmission spectra. Essahlaoui A, Essaoudi H, Hallaoui A, Bouhadda M, Labzour A, Housni A. Journal of Materials and Environmental Sciences, (2018), **Vol.9(1), pg. 228-234**
27. Characterization of inhomogeneous dielectric films by spectroscopic ellipsometry Rivory J. Thin Solid Films, (1998), **Vol.313, pg. 333-40.**
28. Optical Properties of Nonstoichiometric Tantalum Oxide TaO_x (x < 5/2) According to Spectral-Ellipsometry and Raman-Scattering Data. Kruchinin VN, Volodin VA, Perevalov TV, Gerasimova AK, Aliev VS, Gritsenko VA. Optics and Spectroscopy, (2018), **Vol.124(6), pg. 808-813**
29. Optical properties of nanostructured TiO₂ thin films. Karoui MB, Kaddachi Z, Gharbi RIOP Publishing, In Journal of Physics: Conference Series (2015), **Vol. 596(1), pg. 012012**
30. Determination of the optical parameters of a-Si:H thin films deposited by hot wire-chemical vapour deposition technique using transmission spectrum only. Bakr NA, Funde AM, Waman VS, Kamble MM, Hawaldar RR, Amalnerkar DP, Gosavi SW, Jadkar SR. Pramana-Journal of Physics, (2011), **Vol. 76(3), pg. 519-531.**
31. Determining optical constants of selenium thin films using the envelope method. Tashtoush NM, Alkasassbeh O. American Journal of Applied Sciences, (2013), **Vol.10(2), pg. 164.**